

COPIOUS PRODUCTION OF HARD PHOTONS IN THE e^+e^-
COLLIDING EXPERIMENTS*

Yung Su Tsai
Stanford Linear Accelerator Center
Stanford University, Stanford, California 94305

- p. 2. 1st paragraph, line 19: for " ~ 0.8 " read " ~ -0.8 "
- p. 2. 2nd paragraph, line 24: for "and highly" read "and highly non-"
- p. 4. Sec. II, 1st paragraph, line 3: "by Berend and Kleiss³" read
"by Berend, Gastmans and Wu³"
- p. 19. Substitute Ref. 3 to: F. A. Berends and R. Kleiss, "Distribution
in the Process $e^+e^- \rightarrow \mu^+\mu^-(\gamma)$," DESY 80/66 (1980). The program
calculates the cross section to α^3 using Eq. (2.1). The simple
expression for A given in Eqs. (2.1) through (2.5) was obtained
by F. A. Berends, R. Gastmans and T. T. Wu, University of Leuven
preprint, KUL-TF-79/022 (1979).
- p. 23. Change "Table III" to "Table IV"

* Work supported by the Department of Energy, contract DE-AC03-76SF00515.

Add Table III with the following:

TABLE III

Cross sections for $e^+e^- \rightarrow \mu^+\mu^-\gamma$ calculated according to Eq. (2.36). We use $s = (29 \text{ GeV})^2$, $x_{\min} = k_{\min}/E = 4/14.5$, $\theta_{k\text{emin}} = \theta_{k\mu\text{min}} \equiv \theta_{k\ell\text{min}}$, $s'_{\min} = s(1 - x_{\max})$. ΔR_e and ΔR_μ represent the contributions to R from initial and final state γ emission respectively. We let $\delta_s(s') = 0$ when calculating ΔR_e , ΔR_μ and $\Delta R \equiv \Delta R_e + \Delta R_\mu$. $(\Delta R)_{\text{corr}} \equiv 1.2 \Delta R$ which approximately takes into account the effect of $\delta_s(s')$ given by Table II.

$\theta_{k\ell\text{min}}$	k_{\max} (GeV)	s'_{\min} (GeV ²)	ΔR_e %	ΔR_μ %	ΔR %	$(\Delta R)_{\text{corr}}$ %
20°	13.5	58	2.8	1.2	4.0	4.8
20°	14.0	29	3.4	1.3	4.7	5.6
20°	14.3	11.6	4.1	1.3	5.4	6.5
20°	14.4741	1.5	6.3	1.3	7.6	9.1
10°	13.5	58	3.9	1.7	5.6	6.7
10°	14.0	29	4.7	1.8	6.5	7.8
10°	14.3	11.6	5.8	1.8	7.6	9.1
10°	14.4741	1.5	8.9	1.8	10.7	12.8

COPIOUS PRODUCTION OF HARD PHOTONS IN THE e^+e^-
COLLIDING EXPERIMENTS*

Yung Su Tsai
Stanford Linear Accelerator Center
Stanford University, Stanford, California 94305

ABSTRACT

The phenomenon of copious production of hard photons by the initial e^+ or e^- in the e^+e^- colliding beam is discussed. Approximately one-half unit of R in the total hadronic cross section quoted by the experimenters could be due to this source. An improvement in the evaluation of hard photon emission in the e^+e^- colliding beam experiment is given. Inclusion of higher order effects increases the cross section for $e^+ + e^- \rightarrow \gamma + X$ by about 20% at PEP/PETRA energy.

Submitted to Physical Review D

* Work supported by the Department of Energy, contract DE-AC03-76SF00515.

I. INTRODUCTION

Recently Ritson et al., have investigated the possibility of an excited state of muon by sampling $\mu\mu\gamma$ final state from the MAC detector at PEP at CM energy of $2E = 29$ GeV. They found surprisingly large cross section, namely $0.1 \times \sigma_{ee \rightarrow \mu\mu}$ (lowest order) even at large photon energies ($k > 3$ GeV) and large angle between γ and all leptons ($\theta_{k\ell} > 20^\circ$). Normally one would expect the cross section for such events to be very small, approximately $\alpha\sigma_{ee \rightarrow \mu\mu}$. Furthermore they found that $\mu\gamma$ invariant mass was clustered around 16 GeV, a possible candidate for μ^* . After some calculation we concluded that the standard QED indeed can explain these events. The reason for such a large cross section is that a photon can steal almost all the energy from the initial e^+ or e^- resulting in a very large annihilation cross section. When a photon of energy k is emitted by the initial e^+e^- system, s is changed into $s' = s(1-k/E)$. In this experiment s is $(29)^2$ GeV² and s' can be as small as 1.5 GeV² (for $\theta_{\mu^+\mu^-} > 20^\circ$, $E_{\mu^\pm} > 1$ GeV). The cross section for the annihilation can thus be enhanced by two or three orders of magnitude, which is more than enough to compensate for the smallness of α associated with emission of noninfrared γ at large angles.¹ The invariant mass of $\mu\gamma$ is $[2kE_\mu(1-\cos\theta_{k\mu})]^{1/2}$. Since $k \sim 14$ GeV, $E \sim 5$ GeV, $\langle \cos\theta_{k\mu} \rangle \sim -0.8$ for such events it is easy to understand why the $\mu\gamma$ invariant mass is clustered around 16 GeV.

The mechanism of copious production of high-energy γ described above is also true when the final states are hadrons, electrons and τ 's. In the e^+e^- experiment, an event with a high energy photon and highly non-

colinear pair is most likely classified as hadronic. Hence many events of the type $e^+e^- \rightarrow \gamma X$ with X being hadrons, e^+e^- pair, $\mu^+\mu^-$ pair, $\tau^+\tau^-$ pair are likely counted as hadronic reactions. It is therefore quite possible that about² 0.5 of the quoted value of R is due to highly non-colinear $e^+e^- \rightarrow \gamma X$ events. All these events should be excluded when evaluating R.

As a by-product of this research I also looked into how the cross section for $e^+e^- \rightarrow \gamma X$ was calculated by the experimentalists. A Monte Carlo program provided by Berend and Kleiss³ seems to be the standard tool. The phenomenon of copious emission of hard photons at a large angle is buried in this Monte Carlo program. Some improvement can be made on the program by including higher order effects.⁴ The most distinguished features of the higher order effects are the following two:

1. Inclusion of vacuum polarizations and vertex corrections increases the cross section for $e^+e^- \rightarrow \gamma X$ by about 20% at PEP/PETRA energy.
2. The deviation from the coplanarity of the final state can be evaluated by inclusion of multiple photon emission. For example the final state of the reaction $e^+e^- \rightarrow \mu^+\mu^-\gamma$ forms a plane but the final state of the reaction $e^+e^- \rightarrow \mu^+\mu^-\gamma\gamma$ does not. The deviation from the coplanarity can be approximated by assuming that most of the extra photons emitted are soft and are emitted along the direction of motion of either e^+, e^- , μ^+ or μ^- (peaking approximation).

Both of these effects can be incorporated into the existing Monte Carlo program.

In the modern detectors now being used at PEP and PETRA, practically all the particles in the final states are detected and analyzed. In this

situation the Monte Carlo method is the most logical one to be used in the analysis of data. However analytical expressions showing all the gross features of the problem are often useful in rough estimate of the cross sections as well as selection of various cuts to be used in the Monte Carlo methods. We have derived some simple formulas in Section II for this purpose.

II. CALCULATIONS

A. Lowest Order Calculation

Lowest order cross section for $e^+ + e^- \rightarrow \mu^+ + \mu^- + \gamma$ can be obtained using Feynman diagrams shown in Fig. 1. We shall use an approximate formula given by Berend, Gastmans and Wu³ for the matrix element squared,

$$d\sigma = \frac{4\alpha^3}{s\pi^2} \int \frac{d^3P_3}{2E_3} \frac{d^3P_4}{2E_4} \frac{d^3k}{2k} \delta^4(P_1 + P_2 - P_3 - P_4 - k) A \quad (2.1)$$

with

$$A = \text{MEME} + \text{MUMU} + \text{MEMU} \quad , \quad (2.2)$$

$$\text{MEME} = -\frac{m_e^2}{2s'^2} \left[\frac{t^2 + u^2}{(P_1 \cdot k)^2} + \frac{t'^2 + u'^2}{(P_2 \cdot k)^2} \right] + \frac{t^2 + t'^2 + u^2 + u'^2}{4s'(P_1 \cdot k)(P_2 \cdot k)} \quad (2.3)$$

$$\text{MUMU} = -\frac{m_\mu^2}{2s^2} \left[\frac{t^2 + u'^2}{(P_3 \cdot k)^2} + \frac{t'^2 + u^2}{(P_4 \cdot k)^2} \right] + \frac{t^2 + t'^2 + u^2 + u'^2}{4s(P_3 \cdot k)(P_4 \cdot k)} \quad (2.4)$$

$$\begin{aligned} \text{MEMU} &= \frac{t^2 + t'^2 + u^2 + u'^2}{4ss'} \\ &\times \left[-\frac{t}{(P_2 \cdot k)(P_4 \cdot k)} - \frac{t'}{(P_1 \cdot k)(P_3 \cdot k)} + \frac{u'}{(P_1 \cdot k)(P_4 \cdot k)} + \frac{u}{(P_2 \cdot k)(P_3 \cdot k)} \right] \quad (2.5) \end{aligned}$$

and

$$\begin{aligned}
 t &= (P_2 - P_4)^2, & t' &= (P_1 - P_3)^2, & u &= (P_2 - P_3)^2, \\
 u' &= (P_1 - P_4)^2, & s &= (P_1 + P_2)^2, & s' &= (P_3 + P_4)^2.
 \end{aligned}$$

P_1, P_2, P_3 and P_4 refer to four momenta of e^-, e^+, μ^- and μ^+ respectively.

We have also calculated the exact expression for A using Hearn's REDUCE program.⁵ The exact expression for A is about one hundred times more complicated than Eqs. (2.2)-(2.5) but numerically the latter yields results accurate to within one part in 3000 compared with the exact α^3 calculation in the kinematical range we have checked. The MEMU term comes from the interference $(M1 + M2)^+(M3 + M4)$, which is odd under the exchange $\mu^+ \leftrightarrow \mu^-$ and thus it contributes only to the asymmetry and not to the total cross section.

B. Radiative Corrections

We consider next the radiative correction to Eq. (2.1). One inserts the vacuum polarization and noninfrared divergent part of the vertex correction to diagrams M1, M2, M3, M4 in Fig. 1. This correction changes A in Eqs. (2.1)-(2.2) into

$$A' = \text{MEME} [1 + \delta_s(s')] + \text{MUMU} [1 + \delta_s(s)] + \text{MEMU} [1 + \frac{1}{2} \delta_s(s') + \frac{1}{2} \delta_s(s)]. \quad (2.6)$$

δ_s is the symmetric and noninfrared divergent part of the radiative corrections. It consists of noninfrared part of the vertex correction and the vacuum polarization contributions:

$$\delta_s(s) = \delta_{\text{vert}}^e(s) + \delta_{\text{vert}}^\mu(s) + \delta_{\text{vac}}^e(s) + \delta_{\text{vac}}^\mu(s) + \delta_{\text{vac}}^\tau(s) + \delta_{\text{vac}}^{\text{had}}(s) \quad (2.7)$$

δ_{vert}^e and δ_{vert}^μ are vertex corrections for e and μ vertices respectively:

$$\delta_{\text{vert}}^e(s) = \frac{2\alpha}{\pi} \left(\frac{3}{4} \ln \frac{s}{m_e^2} - 1 + \frac{\pi^2}{6} \right) , \quad (2.8)$$

$$\delta_{\text{vert}}^\mu(s) = \frac{2\alpha}{\pi} \left(\frac{3}{4} \ln \frac{s}{m_\mu^2} - 1 + \frac{\pi^2}{6} \right) . \quad (2.9)$$

The vacuum polarizations can be calculated from⁶ -

$$\delta_{\text{vert}}^X(s) = \frac{s}{2\pi^2\alpha} P \int_{s_{\text{th}}}^{\infty} \frac{\sigma_{ee \rightarrow X}(s') ds'}{s - s'} \quad (2.10)$$

where s_{th} is the threshold value of s for the production of the final state X and P stands for the principal part of the integration. For a lepton pair with mass m , we have $s_{\text{th}} = 4m^2$,

$$\sigma_{ee \rightarrow \ell\ell}(s) = \frac{4\pi\alpha^2}{3s} \beta \frac{3-\beta^2}{2} , \quad \text{with } \beta^2 = 1 - \frac{4m^2}{s} ,$$

and we thus obtain from (2.10),

$$\delta_{\text{vac}}^\ell(s) \equiv f(x) \quad (2.11)$$

with $x = s_{\text{th}}/s$ and

$$f(x) = \frac{2\alpha}{\pi} \left\{ -\frac{5}{9} - \frac{x}{3} + \frac{(1-x)^{\frac{1}{2}}(2+x)}{6} \ln \frac{1+(1-x)^{\frac{1}{2}}}{1-(1-x)^{\frac{1}{2}}} \right\} \quad \text{if } x \leq 1 \quad (2.12)$$

and

$$f(x) = \frac{2\alpha}{\pi} \left\{ -\frac{5}{9} - \frac{x}{3} + \frac{(x-1)^{\frac{1}{2}}(2+x)}{3} \tan^{-1} \frac{1}{(x-1)^{\frac{1}{2}}} \right\} \quad \text{if } x > 1 . \quad (2.13)$$

Since we are interested in energy range $s \gg 4m_\mu^2$, we have

$$\delta_{\text{vac}}^e(s) = \frac{2\alpha}{\pi} \left(\frac{1}{3} \ln \frac{s}{m_e^2} - \frac{5}{9} \right) , \quad (2.14)$$

$$\delta_{\text{vac}}^{\mu}(s) = \frac{2\alpha}{\pi} \left(\frac{1}{3} \ln \frac{s}{m_{\mu}^2} - \frac{5}{9} \right), \quad (2.15)$$

$$\delta_{\text{vac}}^{\tau}(s) = f(x_{\tau}) \quad \text{with } x_{\tau} = \frac{4m_{\tau}^2}{s}. \quad (2.16)$$

Except for resonances, $\sigma_{e^+e^- \rightarrow \text{hadron}}(s)$ can be roughly represented by⁷ $1.2 \sigma_{e^+e^- \rightarrow \text{quarks partons}}$, hence we can write $\delta_{\text{vac}}^{\text{had}}$ in terms of the function $f(x)$ given above in the following way: -

$$\delta_{\text{vac}}^{\text{had}}(s) = 1.2 \left\{ \frac{5}{3} f(x_u) + \frac{1}{3} f(x_s) + \frac{4}{3} f(x_c) + \frac{1}{3} f(x_b) \right\}, \quad (2.17)$$

where x_u, x_s, x_c and x_b are s_{th}/s for production of different quark flavors and are given approximately by $x_u = 4m_{\pi}^2/s$, $x_s = 1 \text{ GeV}^2/s$, $x_c = 9 \text{ GeV}^2/s$ and $x_b = 100 \text{ GeV}^2/s$.

The numerical values of $\delta_{\text{vert}}^e, \delta_{\text{vert}}^{\mu}, \delta_{\text{vac}}^e, \delta_{\text{vac}}^{\mu}, \delta_{\text{vac}}^{\tau}, \delta_{\text{vac}}^{\text{had}}$ and their sum δ_s are given in Table I.

Normally Eq. (2.1) is regarded as part of the radiative corrections to the lowest order cross section for $e^+e^- \rightarrow \mu^+\mu^-$. In this case the higher order effect is usually obtained by exponentiating the infrared divergent part on the lowest order corrections. For example for an experiment in which the only experimental constraint is either $2E - E_3 - E_4 > \Delta E$ or $\sum_{i=1}^{\infty} k_i < \Delta E$ and $\Delta E \ll E$, the cross section for $e^+e^- \rightarrow \mu^+\mu^-$ + any number of photons can be written as⁸

$$\frac{d\sigma}{d\Omega_3} = \frac{d\sigma_0}{d\Omega_3} \left(1 + \delta_s + \delta_A \right) \left(\frac{\Delta E}{E} \right)^T, \quad (2.18)$$

where $d\sigma_0/d\Omega_3$ is the lowest order differential cross section for $e^+e^- \rightarrow \mu^+\mu^-$,

$$\frac{d\sigma_0}{d\Omega_3} = \frac{\alpha^2}{4s} \left(1 + \cos^2\theta \right). \quad (2.19)$$

$(\Delta E/E)^T$ is the infrared divergent part of the radiative corrections and hence it was exponentiated in order to take care of multiple soft photon emission.

$$T = t_e + t_\mu + t_{e\mu} \quad , \quad (2.20)$$

$$t_e = \frac{2\alpha}{\pi} \left(\ln \frac{s}{m_e^2} - 1 \right) \quad , \quad (2.21)$$

$$t_\mu = \frac{2\alpha}{\pi} \left(\ln \frac{s}{m_\mu^2} - 1 \right) \quad , \quad (2.22)$$

$$t_{e\mu} = \frac{8\alpha}{\pi} \ln \left(\tan \frac{\theta}{2} \right) \quad , \quad (2.23)$$

where θ is the angle between e^- and μ^- . $t_{e\mu}$ is asymmetric with respect to the plane perpendicular to the beam axis. δ_A is the asymmetric and noninfrared divergent part of the radiative corrections:

$$\begin{aligned} \delta_A(\theta) = \frac{2\alpha}{\pi} \left\{ \frac{-2}{1+\cos^2\theta} \left[\cos\theta \left\{ \ln^2\left(\sin\frac{\theta}{2}\right) + \ln^2\left(\cos\frac{\theta}{2}\right) \right\} + \sin^2\frac{\theta}{2} \ln\left(\cos\frac{\theta}{2}\right) \right. \right. \\ \left. \left. - \cos^2\frac{\theta}{2} \ln\left(\sin\frac{\theta}{2}\right) \right] + 2 \ln^2\left(\sin\frac{\theta}{2}\right) - 2 \ln^2\left(\cos\frac{\theta}{2}\right) \right. \\ \left. - \Phi\left(\sin^2\frac{\theta}{2}\right) + \Phi\left(\cos^2\frac{\theta}{2}\right) \right\} \quad , \quad (2.24) \end{aligned}$$

where $\Phi(x)$ is the Spence function (also called dilogarithm). The numerical values of $\delta_A(\theta)$ are shown in Table II. δ_A and $t_{e\mu}$ are both odd with respect to the interchange $\mu^+ \leftrightarrow \mu^-$ and hence contribute only to the asymmetry but not to the total cross section up to order α^3 in the cross section. Their product $\delta_A t_{e\mu}$ will contribute to the total cross section in the α^4 cross section, but its contribution to $e^+e^- \rightarrow \mu^+\mu^-\gamma$ is less than 1% if $10^\circ < \theta < 170^\circ$. This can be seen

from

$$\frac{|\delta_A t_{e\mu}|}{t_e + t_\mu} < 0.01 \quad \text{if } 10^0 < \theta \quad \text{for } s = 900 \text{ GeV}^2 \quad . \quad (2.25)$$

Since δ_s is about 20%, the contribution to the cross section from $\delta_A t_{e\mu}$ can be ignored unless one is interested in a very small angle.

The asymmetric terms δ_A and $t_{e\mu}$ are very important when one is dealing with the effects due to interference between Z_0 and γ exchanges. Also at PEP/PETRA energies ($s \sim 1000 \text{ GeV}^2$) the weak-electromagnetic interference is about s/M_W^2 of the pure electromagnetic effect; hence it is comparable to the α^2 radiative corrections which is $O(\alpha^2 \ln^2 s/m_e^2)$. The corrections to this order have never been calculated. We shall not deal with this effect in this paper. Therefore we shall ignore the asymmetric terms $t_{e\mu}$ and δ_A in Eq. (2.18) and Eq. (2.20), as well as MEMU in Eq. (2.5) and Eq. (2.6).

Equation (2.18) is correct only when $k/E \ll 1$. If we ignore the asymmetric terms δ_A and $t_{e\mu}$, Eq. (2.18) can be generalized to hard photon emission in the following way:

Since ΔE represents the maximum energy of a photon which can be emitted, differentiating Eq. (2.18) with respect to ΔE yields

$$\frac{d\sigma}{d\Omega_3 dx} = \frac{d\sigma_0}{d\Omega_3} \left(1 + \delta_s + \delta_A \right) \frac{T}{x} x^T \quad (2.26)$$

where $x = k/E$. $(d\sigma_0/d\Omega_3) (T/x)$ represents the lowest order bremsstrahlung cross section for small x . δ_s is the corrections due to the insertion of vacuum polarizations and noninfrared part of the vertex correction. As shown in Eq. (2.6) one should use $\delta_s(s')$ when a hard

photon is emitted by the initial state but $\delta_s(s)$ when the photon is emitted by the final state. The factor x^T represents the effect of multiple photon emission. Ignoring the asymmetric term, $T_{e\mu}$, we decompose x^T into four factors $x^T = x^{t_1} x^{t_2} x^{t_3} x^{t_4}$, where

$$t_1 = t_2 = \frac{\alpha}{\pi} \left[\ln \left(\frac{s}{m_e^2} \right) - 1 \right] \quad (2.27)$$

and

$$t_3 = t_4 = \frac{\alpha}{\pi} \left[\ln \left(\frac{s'}{m_\mu^2} \right) - 1 \right] \quad (2.28)$$

It is convenient to regard t_1 , t_2 , t_3 and t_4 as the thicknesses of the equivalent radiators⁴ in the paths of p_1 , p_2 , p_3 and p_4 particles, respectively. These equivalent radiators simulate the effect of multiple photons emitted by p_1 , p_2 , p_3 and p_4 , respectively. A monoenergetic particle initially with energy E_i after going through a radiator of thickness t_i (in unit of radiation lengths) will acquire an energy distribution ($i = 1, 2, 3, 4$)

$$\rho_i(x_i) dx_i = t_i (1-x_i)^{t_i-1} dx_i \quad (2.29)$$

where

$$x_i = \frac{E'_i}{E_i} \quad .$$

Integrating $\rho_i(x_i)$ from 0 to $\Delta E/E_i$ we have

$$\int_0^{\Delta E/E_i} \rho_i(x_i) dx_i = \left(\frac{\Delta E}{E_i} \right)^{t_i} \quad (2.30)$$

Equation (2.29) is accurate only when $1-x_i \ll 1$. For a large energy loss a better approximation for the internal bremsstrahlung from a

spin- $\frac{1}{2}$ particle is^{1,4}

$$\rho_i(x_i) = t_i \frac{1+x_i^2}{2} (1-x_i)^{t_i-1} \quad . \quad (2.31)$$

The final state of the reaction $e^+e^- \rightarrow \mu^+\mu^-\gamma$ is coplanar in the CM system. If more than one photon is emitted, the final state is no longer coplanar unless the extra photons are parallel to μ^- , μ^+ or the original γ . Since most of the photons are emitted along either e^+ , e^- , μ^- or μ^+ , the extra photons emitted by e^+ or e^- are the major sources of acoplanarity. Thus in order to choose the acoplanarity cuts one has to understand the effect of t_1 and t_2 which simulates the effect of multiple photon emission by e^- and e^+ , respectively. This can be done easily in the Monte Carlo program by replacing the monochromatic initial energies E_1 and E_2 by distributions given by Eq. (2.31), the rest of the calculation uses the perturbation theory for evaluating $e^+e^- \rightarrow \mu^+\mu^-\gamma$ [i.e., Eq. (2.6)].

C. Partially Integrated Cross Sections

With the modern detectors now being used at PEP and PETRA, practically all the particles in the final state are detected and analyzed. It is therefore difficult and probably not useful to decide which variables in Eq. (2.1) should be integrated analytically. For this reason the Monte Carlo method is the most logical choice for analyzing the data. However it is dangerous to rely solely on the Monte Carlo method without understanding the gross features. We derive some partially integrated cross sections showing these gross features of the cross section. There are several regions in the phase space of $\mu^+\mu^-\gamma$ where the events are concentrated.

1. Soft Photon Region. The probability of emitting a soft photon is proportional to dk/k^{1-T} (see Eq. (2.26)).

2. Hard Photon Region. When a hard photon is emitted by the initial electron or positron, the resultant annihilation cross section is enhanced by the factor $s/s' = (1-k/E)^{-1}$. This factor can be very large as mentioned in the introduction (see Eq. (2.3)). Thus near $k = E$, the cross section has k dependence of the form $dk/(1-k/E)$.

3. Small Emission Angles. Photons are predominantly emitted along either p_1, p_2, p_3 or p_4 as can be seen from the denominators $p_1 \cdot k, p_2 \cdot k, p_3 \cdot k$ and $p_4 \cdot k$ in Eqs. (2.2), (2.3) and (2.4). Let us consider the emission of γ by the initial e^+e^- ; this is given by MEME in Eq. (2.3). The term proportional to m_e^2 is negative and is important only when the emission angle is small compared with m_e/E . The second term dominates the cross section when θ_{k1} and θ_{k2} are large compared with m_e/E . Since $p_1 = -p_2$, we have

$$\frac{1}{(p_1 \cdot k)(p_2 \cdot k)} = \frac{1}{k^2(E_1^2 - p_1^2 \cos^2 \theta_{k1})} = \frac{1}{k^2(m_e^2 + p_1^2 \sin^2 \theta_{k1})} \quad (2.32)$$

This shows that when $\theta_{k1} \gg m_1/E_1$ the cross section is independent of m_e and the angular dependence is $(d \cos \theta_{k1})/\sin^2 \theta_{k1}$. The emission of γ from the final muons is given by MUMU in Eq. (2.4). Here p_3 and p_4 are no longer opposite to each other but the dependence of the cross sections on the emission angle is roughly the same as that for the electrons except here we replace m_e by m_μ .

We derive an approximate analytic expression showing all these three characteristic features in the following. Let us consider MEME

term in Eqs. (2.1) and (2.3). We first perform integration with respect to p_3 and p_4 in the rest frame of $p_3 + p_4$ with the help of δ^4 function, then we perform the integration with respect to k in the laboratory system from k_{\min} to k_{\max} and the angle between k and p_1 from $\theta_{kl\min}$ to $\pi - \theta_{kl\min}$. The result is

$$\sigma_{ee \rightarrow \gamma X}(s) = \frac{2\alpha}{\pi} \int_{x_{\min}}^{x_{\max}} \left[-\frac{(1-x) \cos \theta_{kl\min}}{1+\gamma^2 \sin^2 \theta_{kl\min}} + \frac{1+(1-x)^2}{2} \right. \\ \left. \times \ln \frac{\gamma^2 (1 + \cos \theta_{kl\min})^2}{1+\gamma^2 \sin^2 \theta_{kl\min}} \right] \sigma_{ee \rightarrow X}(s') (1 + \delta_s(s')) \frac{dx}{x^{1-t_1-t_2}} \quad (2.33)$$

where $x = k/E_1$, $\gamma = E_1/m_e$, and $\sigma_{ee \rightarrow X}(s')$ is the lowest order cross section for the process $e^+e^- \rightarrow X$ as a function of $s' = s(1-x)$. For muon pair we have

$$\sigma_{ee \rightarrow \mu\mu}(s') = \frac{4\pi\alpha^2}{3s(1-x)} .$$

$\delta_s(s')$ is the correction due to vacuum polarizations and the noninfrared part of vertex corrections as shown in Eq. (2.7). The factor dx/x was replaced by $dx/x^{1-t_1-t_2}$ in order to account for the infinitely many soft photons emitted by p_1 and p_2 . We have ignored the γ emission by the final particles, hence this formula is appropriate for use in calculating the cross section for $e^+e^- \rightarrow \gamma + \text{hadrons}$ due to emission of γ from the initial e^\pm . The cross section for emission of γ from the final μ^\pm can be inferred from Eq. (2.33).

We can write approximately

$$\begin{aligned}
 \sigma_{ee \rightarrow \mu\mu\gamma}(s) = & \sigma_{ee \rightarrow \mu\mu}(s) \frac{2\alpha}{\pi} \int_{x_{\min}}^{x_{\max}} \left\{ \left[-\frac{\cos\theta_{kemin}}{1 + \gamma_e^2 \sin^2\theta_{kemin}} + \frac{1 + (1-x)^2}{2(1-x)} \right. \right. \\
 & \times \ln \left. \left. \frac{\gamma_e^2 (1 + \cos\theta_{kemin})^2}{1 + \gamma_e^2 \sin^2\theta_{kemin}} \right] (1 + \delta_s(s')) \right. \\
 & + \left. \left[-\frac{\cos\theta_{k\mu min} (1-x)}{1 + \gamma_\mu^2 \sin^2\theta_{k\mu min}} + \frac{(1 + (1-x)^2)}{2} \ln \frac{\gamma_\mu^2 (1 + \cos\theta_{k\mu min})^2}{1 + \gamma_\mu^2 \sin^2\theta_{k\mu min}} \right] \right. \\
 & \left. \times (1 + \delta_s(s)) \right\} \frac{dx}{x^{1-t_1-t_2-t_3-t_4}} \quad (2.34)
 \end{aligned}$$

The first square bracket comes from the γ emission by the initial e^\pm and the second square bracket comes from the emission of γ by the final μ^\pm . θ_{kemin} and $\theta_{k\mu min}$ are respectively γe and $\gamma\mu$ angular cuts. As shown in Table II, $\delta_s(s')$ is a very slowly changing function of x , and hence we may approximate it by its average value. If we are not interested in very small values of x_{\min} , the correction due to multiple photon emission can be ignored (i.e., $t_1 + t_2 + t_3 + t_4 \rightarrow 0$). Equation (2.34) can then be integrated, yielding

$$\begin{aligned}
 \Delta R_{\mu\mu\gamma} &\equiv \frac{\sigma_{ee\rightarrow\mu\mu\gamma}(s)}{\sigma_{ee\rightarrow\mu\mu}(s)} \\
 &= \frac{2\alpha}{\pi} \left\{ \left[-\frac{\cos\theta_{kemin}}{1+\gamma_e^2 \sin^2\theta_{kemin}} \ln \frac{x_{max}}{x_{min}} + \left(\ln \frac{x_{max}}{x_{min}} - \frac{x_{max}-x_{min}}{2} \right) \right. \right. \\
 &\quad \left. \left. + \frac{1}{2} \ln \frac{1-x_{max}}{1-x_{min}} \right) \ln \frac{\gamma_e^2 (1+\cos\theta_{kemin})^2}{1+\gamma_e^2 \sin^2\theta_{kemin}} \right] (1+\delta_s(s'_{ave})) \\
 &\quad + \left[-\frac{\cos\theta_{kumin}}{1+\gamma_\mu^2 \sin^2\theta_{kumin}} \left\{ \ln \frac{x_{max}}{x_{min}} - (x_{max} - x_{min}) \right\} \right. \\
 &\quad \left. + \left\{ \ln \frac{x_{max}}{x_{min}} - (x_{max} - x_{min}) + \frac{x_{max}^2 - x_{min}^2}{4} \right\} \right. \\
 &\quad \left. \times \ln \frac{\gamma_\mu^2 (1+\cos\theta_{kumin})^2}{1+\gamma_\mu^2 \sin^2\theta_{kumin}} \right] (1+\delta_s(s)) \left. \right\} \quad (2.35)
 \end{aligned}$$

When the emission angles are made large enough such that $\gamma_\mu \theta_{kumin} \gg 1$ and $\gamma_e \theta_{kemin} \gg 1$, we have

$$\begin{aligned}
 \Delta R_{\mu\mu\gamma} &\rightarrow \frac{4\alpha}{\pi} \left\{ \left[\ln \frac{x_{max}}{x_{min}} - \frac{x_{max}-x_{min}}{2} + \frac{1}{2} \ln \frac{s'_{max}}{s'_{min}} \right] (1+\delta_s(s'_{ave})) \right. \\
 &\quad \times \ln \cot \frac{\theta_{kemin}}{2} + \left[\ln \frac{x_{max}}{x_{min}} - (x_{max} - x_{min}) + \frac{x_{max}^2 - x_{min}^2}{4} \right] \\
 &\quad \left. \times (1+\delta_s(s)) \ln \cot \frac{\theta_{kumin}}{2} \right\} \quad (2.36)
 \end{aligned}$$

We have used the relation $s' = s(1-x)$ to write $\ln[(1-x_{max})/(1-x_{min})] = \ln(s'_{min}/s'_{max})$ in order to make it apparent that this log is due to the singularity in s' . Experimentally s' is the square of the invariant mass of μ pair and hence it can be measured more accurately than the

energy of γ . $\delta_s(s'_{ave})$ is roughly 20% as shown in Table II. It is interesting to observe that Eq. (2.36) is independent of m_e , m_μ and E_i 's except in $\delta_s(s)$ which varies with s very slowly.

III. NUMERICAL EXAMPLES

In Table III we show some numerical examples of cross sections for $(e^+e^- \rightarrow \mu^+\mu^-\gamma)/(4\alpha^2\pi/3s)$ calculated according to Eq. (2.36). θ_{klmin} is the angular cut between γ and leptons (e or μ). The parameters used corresponds to the actual case used by the MAC detector group at PEP. We have shown both k_{max} and s'_{min} ; they are related by $s'_{min} = s(1-k_{max}/E)$. These two columns illustrate why it is sometimes dangerous to use a Monte Carlo program blindly. Usually the energy resolution of the photon detector is not good enough to specify the exact k_{max} shown in the table. Thus one can easily make a factor of two error in evaluating the cross section by specifying the wrong k_{max} . s'_{min} can be more accurately determined and in the MAC experiment $s'_{min} = 1.5 \text{ GeV}^2$ is the actual cut.⁹ ΔR_e and ΔR_μ represent the contributions to R from initial and final state γ emission, respectively. We let $\delta_s(s') = 0$ when calculating ΔR_e and ΔR_μ and $\Delta R \equiv \Delta R_e + \Delta R_\mu$. $(\Delta R)_{corr} \equiv 1.2 \times R$ which approximately takes into account the effect of $\delta_s(s')$ given in Table II.

The copious production of high-energy γ has experimental consequences on experiments using the small angle detector (2γ experiment) as well as the measurement of R using the central detectors. In Table IV we compute $\sigma(ee \rightarrow \gamma X)/\sigma(ee \rightarrow X) \equiv \Delta R/R$ using only the first half of Eq. (2.36). X can be e^+e^- , $\mu^+\mu^-$, $\tau^+\tau^-$, or hadrons. Experimentally these events are characterized by one very high-energy photon and on the opposite side

either two charged particles or two jets of hadrons. These events tend to be lumped as the hadronic events when evaluating $R = \sigma(ee \rightarrow \text{hadrons}) / \sigma(ee \rightarrow \mu^+ \mu^-)$. From Table IV we see that roughly one unit of R in total cross section for small angle detector ($\theta > 1.5^\circ$) could be due to $ee \rightarrow \gamma X$, the detail depends upon θ_{kemin} and s'_{min} . Similarly approximately one-half unit in R in the central detector ($\theta > 10^\circ$) could be due to $ee \rightarrow \gamma X$. Since the value of R is used for the test of QCD, we believe a more careful subtraction of $ee \rightarrow \gamma X$ events should be exercised. There are two ways of handling this problem. One way is to identify all such events and discard them. The other is to include all these events and make theoretical estimates of their cross sections and to subtract them from the data. Probably some combination of the two methods is the ideal solution.

Acknowledgment

The author wishes to thank David Ritson who insisted that the author look into this problem thoroughly. I would also like to thank Don Groom, William T. Ford and David Ritson for discussions on the detail of the experiment done by the MAC detector. Thanks are also due to Dan Scharre who showed me the result of his Monte Carlo calculation.

Footnotes and References

1. A similar phenomenon occurs in the electron scattering from a stationary target. Rutherford cross section is proportional to $1/E^2$ of the incident energy. An incident electron can emit a very hard photon losing practically all its energy and then gets scattered by a nucleus at a low energy with a large cross section. This results in a rise in the radiative tail at the low energy end of the scattered electron spectrum. See L. W. Mo and Y. S. Tsai, Rev. Mod. Phys. 41, 205 (1969). Also Y. S. Tsai, "Radiative Correction to Electron Scattering," SLAC-PUB-848 (1971).
2. Since the $\mu\mu\gamma$ final states alone contribute about 0.1 to R we expect that the total contributions from $ee \rightarrow \gamma X$ for X being e^+e^- , $\mu^+\mu^-$, $\tau^+\tau^-$ and hadrons should be roughly 0.5.
3. F. A. Berends and R. Kleiss, "Distribution in the Process $e^+e^- \rightarrow \mu^+\mu^-(\gamma)$," DESY 80/66 (1980). The program calculates the cross section to α^3 using Eq. (2.1). The simple expression for A given in Eqs. (2.1) through (2.5) was obtained by F. A. Berends, R. Gastmans and T. T. Wu, University of Leuven preprint, KUL-TF-79/022 (1979).
4. A similar method of dealing with higher order effects in electron scattering was treated in Y. S. Tsai, "Radiation Corrections to Electron Scattering," SLAC-PUB-848 (1971) unpublished.
5. A. C. Hearn, "REDUCE 2 User's Manual," Stanford Artificial Intelligence Project, MEMO AIM-133 (1970).
6. Y. S. Tsai, Phys. Rev. 120, 269 (1960).
7. The factor 1.2 is an empirical factor which presumably can be explained by QCD.

8. The first person to suggest the exponentiation of the lowest order radiative corrections is J. Schwinger, Phys. Rev. 76, 760 (1949). D. R. Yennie, S. C. Frautschi and H. Suura, Ann. Phys. (NY) 13, 379 (1961) showed that only the infrared divergent part should be exponentiated. The asymmetric term $t_{e\mu}$ was first obtained by Y. S. Tsai in "Proceedings of the International Symposium on Electron and Photon Interactions at High Energies," Hamburg (1965), Vol. II, P. 392. The expression for $\delta_A(\theta)$ was obtained by I. B. Khriplovich, Sov. J. Nucl. Phys. 17, 298 (1973), D. A. Discus, Phys. Rev. D8, 890 (1973), R. W. Brown et al., Phys. Lett. 43B, 403 (1973).
9. D. Ritson, private communication.

TABLE I

Noninfrared and Asymmetric part of the radiative correction $\delta_A(\theta) = -\delta_A(\pi - \theta)$. This function is independent of energy in the extreme relativistic limit. θ is defined as the angle between e^- and μ^- .

θ (degree)	δ_A (percent)
1	9.0
2	6.5
3	5.2
5	3.9
10	2.4
20	1.3
30	0.8
40	0.5
50	0.3
60	0.2
70	0.1
80	0.1
90	0

TABLE II

Corrections due to vertex corrections and the vacuum polarizations in percent. δ_s is the sum of all these corrections.

\sqrt{s} GeV	δ_{vert}^e	δ_{vert}^μ	δ_{vac}^e	δ_{vac}^μ	δ_{vac}^τ	$\delta_{\text{vac}}^{\text{had}}$	δ_s
1	5.6	1.9	2.1	0.4	-0.0	0.5	10.4
5	6.7	3.0	2.6	0.9	-0.1	1.9	15.0
10	7.2	3.5	2.8	1.2	0.2	2.7	17.6
20	7.7	4.0	3.0	1.4	0.5	3.8	20.3
29	7.9	4.2	3.1	1.5	0.6	4.3	21.7
34	8.0	4.3	3.2	1.5	0.7	4.6	22.3
50	8.3	4.6	3.3	1.7	0.8	5.1	23.7
100	8.8	5.1	3.5	1.9	1.0	6.0	26.3
200	9.3	5.6	3.7	2.1	1.2	7.0	28.8

TABLE III

Cross sections for $e^+e^- \rightarrow \mu^+\mu^-\gamma$ calculated according to Eq. (2.36). We use $s = (29 \text{ GeV})^2$, $x_{\min} = k_{\min}/E = 4/14.5$, $\theta_{k\text{emin}} = \theta_{k\mu\text{min}} \equiv \theta_{k\ell\text{min}}$, $s'_{\min} = s(1 - x_{\max})$. ΔR_e and ΔR_μ represent the contributions to R from initial and final state γ emission respectively. We let $\delta_s(s') = 0$ when calculating ΔR_e , ΔR_μ and $\Delta R \equiv \Delta R_e + \Delta R_\mu$. $(\Delta R)_{\text{corr}} \equiv 1.2 \Delta R$ which approximately takes into account the effect of $\delta_s(s')$ given by Table II.

$\theta_{k\ell\text{min}}$	k_{\max} (GeV)	s'_{\min} (GeV ²)	ΔR_e %	ΔR_μ %	ΔR %	$(\Delta R)_{\text{corr}}$ %
20°	13.5	58	2.8	1.2	4.0	4.8
20°	14.0	29	3.4	1.3	4.7	5.6
20°	14.3	11.6	4.1	1.3	5.4	6.5
20°	14.4741	1.5	6.3	1.3	7.6	9.1
10°	13.5	58	3.9	1.7	5.6	6.7
10°	14.0	29	4.7	1.8	6.5	7.8
10°	14.3	11.6	5.8	1.8	7.6	9.1
10°	14.4741	1.5	8.9	1.8	10.7	12.8

TABLE IV

Calculation of $\Delta R/R \equiv \sigma(ee \rightarrow \gamma X)/\sigma(ee \rightarrow X)$ using the first half of Eq. (2.36). We assume $\sigma(ee \rightarrow X) \propto s^{-1}$ and $x_{\min} = 0.1$.

θ_{kemin} is the cut for angle between γ and e. s'_{\min} is related to x_{\max} by $x_{\max} = 1 - s'_{\min}/s$ with $s = (29 \text{ GeV})^2$

s'_{\min} (GeV ²)	θ_{kemin}			
	1.5°	10°	20°	30°
1	20.8 ^a	11.7	8.3	6.3
4×10^{-2}	27.3	15.3	10.9	8.3
10^{-6}	48.8	27.4	19.5	14.8

^aThe values of $\Delta R/R$ given are in percent.

Figure Caption

Fig. 1. Lowest order Feynman diagrams for the process $e^+e^- \rightarrow \mu^+\mu^-\gamma$.

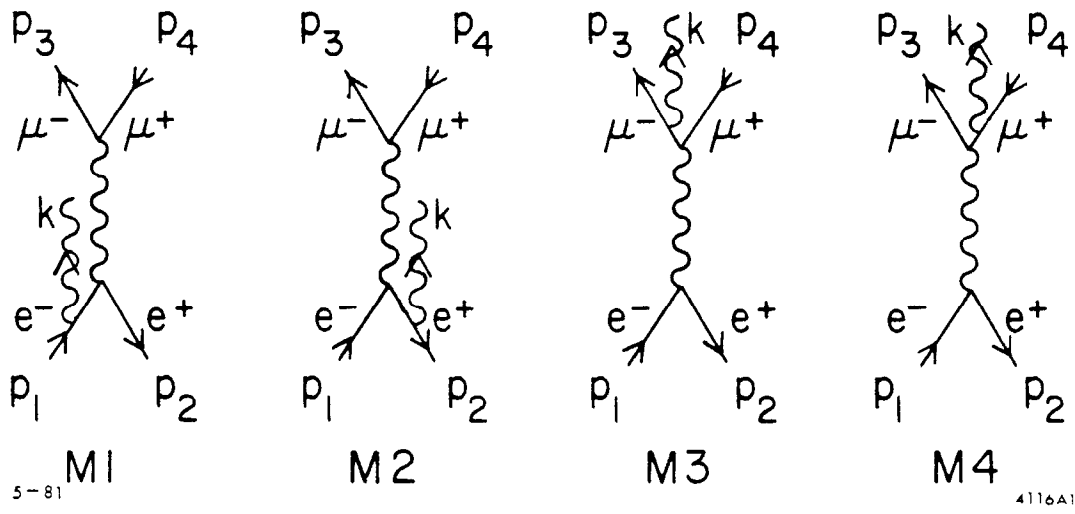


Fig. 1